Dynamics of Bloch oscillations in disordered lattice potentials

T. Schulte,[1,2] S. Drenkelforth,[1] G. Kleine Büning,[1] W. Ertmer,[1] J. Arlt,[1,*] M. Lewenstein,[2,3] and L. Santos[4]
[1]*Institut für Quantenoptik, Leibniz Universität Hannover, Welfengarten 1, D-30167 Hannover, Germany*
[2]*ICFO—Institut de Ciències Fotòniques, E-08860 Castelldefels (Barcelona), Spain*
[3]*ICREA—Institució Catalana de Recerca i Estudis Avançats, E-08010 Barcelona, Spain*
[4]*Institut für Theoretische Physik, Leibniz Universität Hannover, D-30167 Hannover, Germany*
(Received 20 July 2007; published 6 February 2008)

We present a detailed analysis of the dynamics of Bloch oscillations of Bose-Einstein condensates in disordered lattice potentials. Due to the disorder and the interparticle interactions these oscillations undergo a dephasing, reflected in a damping of the center of mass oscillations, which should be observable under realistic experimental conditions. The interplay between interactions and disorder is far from trivial, ranging from an interaction-enhanced damping due to modulational instability for strong interactions, to an interaction-reduced damping due to a *dynamical screening* of the disorder potential.

DOI: 10.1103/PhysRevA.77.023610 PACS number(s): 03.75.Lm, 03.75.Kk, 64.60.Cn

Bloch oscillations (BOs) constitute one of the most fundamental quantum phenomena for particles in periodic potentials. Under the influence of a constant force, particles in such potentials undergo an oscillatory motion instead of being linearly accelerated [1,2]. Although BOs are strongly linked to the dynamics of electrons in solids, they have not been observed in bulk crystalline materials so far, since lattice imperfections such as defects and phonons damp the coherent electronic motion before a single BO cycle is completed. The first observation of BOs was achieved in so-called semiconductor superlattices [3], which exhibit much larger periodicities. However, disorder also leads to a fast decay of the BOs in these systems.

On the contrary, ultracold gases in optical lattices provide perfect periodic potentials, with neither defects nor phonons. As a consequence, these systems open unprecedented possibilities for the detailed analysis of quantum transport in lattices, and in particular for the observation of BOs with very long lifetimes [4]. However, in spite of their perfect periodicity, optical lattices allow for the controlled introduction of different types of disorder [5–8]. Recent experiments have analyzed the effects of controlled disorder on the properties of ultracold gases [10–15]. These experiments have clearly shown that ultracold gases are indeed very promising systems for the analysis of the intriguing interplay between disorder and interparticle interactions.

This paper is devoted to the analysis of this interplay in the BO dynamics of Bose-Einstein condensates (BECs) in tilted optical lattices. The dynamics of BOs is usually analyzed in terms of the Wannier-Stark (WS) energy ladder in such systems. Any disorder introduces an unequal spacing in this ladder and thus leads to a damping of the BOs. In addition, the BOs are nontrivially modified by the interactions in the system. Strong interactions enforce damping, due to dynamical instability. However, weak interactions can cause a *dynamical screening* of the disorder potential, prolonging the lifetime of the BOs [16]. Although quasi-one-dimensional systems allow for a qualitative understanding of the physics involved, in typical experimental conditions radial excitations play a non-negligible role. In this paper we therefore first develop a qualitative understanding of the dynamics of BOs in the one-dimensional (1D) case and then extend our analysis to the experimentally relevant 3D case. Finally, we discuss a method for the observation of damped BOs by analyzing the momentum distribution in time-of-flight (TOF) measurements.

Consider the quasi-1D case, in which a BEC at low temperature is so strongly confined by a harmonic trap of frequency $\omega_\perp$ in the xy plane that the chemical potential μ is much smaller than the transverse level spacing $\mu \ll \hbar\omega_\perp$. Under these conditions, the 1D dynamics of the condensate wave function Φ along the z axis is given by the Gross-Pitaevskii-equation (GPE) [17],

$$i\hbar\partial_t\Phi = \left[\frac{-\hbar^2}{2m}\frac{\partial^2}{\partial z^2} + V(z) + g|\Phi|^2\right]\Phi, \tag{1}$$

where m denotes the atomic mass, and $g=4\pi a_s\hbar\omega_\perp$ is the 1D coupling constant, with a_s the s-wave scattering length. $V(z)$ denotes an external potential of the form

$$V(z) = m\omega^2 z^2/2 + sE_r \sin^2(\bar{k}z) - Fz + V_{dis}(z), \tag{2}$$

i.e., a superposition of an axial harmonic trap with frequency ω, a tilted potential with slope F, a disorder potential $V_{dis}(z)$, and a lattice potential of periodicity $d=\pi/\bar{k}$, and depth s in units of the recoil energy $E_r=\hbar^2\bar{k}^2/2m$. The condensate ground state in the superimposed harmonic and lattice potential serves as the initial state for our simulations of the dynamics.

Figure 1 shows the averaged position $\langle z(t)\rangle = \int dz \Phi^* z \Phi$ for a rubidium condensate, with $\omega_\perp = 2\pi \times 200$ Hz, $d=412.5$ nm, $s=5$, and $Fd/E_r=0.05$, for different particle numbers N, axial trap frequencies ω, and disorder depths. As disorder potential, we consider Gaussian noise with correlation length $L \simeq 3.3$ μm [9]. We define the disorder depth V_Δ as twice the standard deviation from its mean value, according to [10,12], which merely adds an offset to the potential. Figure 1 demonstrates that even for situations where interac-

*arlt@iqo.uni-hannover.de

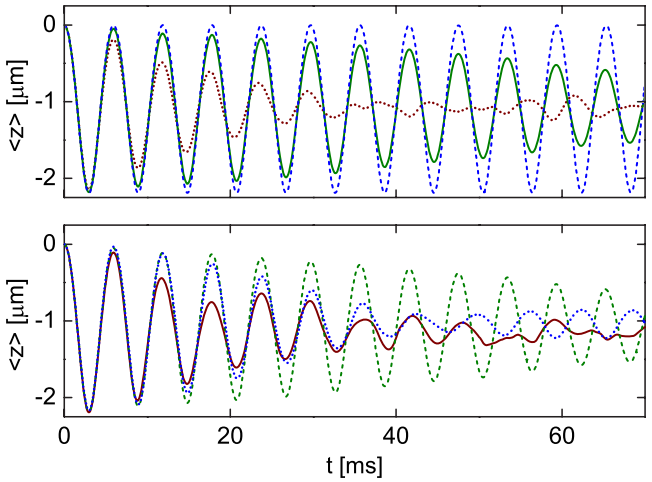

FIG. 1. (Color online) Averaged position of a BEC undergoing BOs. Top frame: $N=350$ particles, $\omega=7$ Hz, and disorder depths $V_\Delta/E_r=0$ (dashed), 0.02 (solid), and 0.04 (dotted). Bottom frame: $V_\Delta/E_r=0.02$ for the noninteracting case, $\omega=3.5$ Hz (dotted), $N=350$, $\omega=7$ Hz (dashed), and $N=700$, $\omega=10$ Hz (solid). The trap frequencies were adjusted to match the initial wave-packet widths.

tions are negligible ($N=1$) disorder induces strong BO damping. The role of the interactions is far from trivial, as shown in Fig. 1, since they may enhance or significantly reduce the BO damping. We analyze this intriguing physics in detail below.

The BO damping can be understood from a simplified analysis in the tight-binding regime. In this regime, we may project the condensate wave function into the Wannier basis of localized states $|n\rangle$, where n labels the lattice sites. $\Phi_n \equiv \langle n|\Phi\rangle$ is provided by the discrete nonlinear Schrödinger equation (DNLSE) [18],

$$i\hbar\dot{\Phi}_n = \hat{H}_0\Phi_n + \epsilon_n\Phi_n + U|\Phi_n|^2\Phi_n, \tag{3}$$

where ϵ_n denotes the external (possibly disordered) potential and U is the on-site interaction energy. $\hat{H}_0$ is the Hamiltonian for the tilted lattice in the absence of both disorder and interactions, $\hat{H}_0\Phi_n=-J\Sigma_n(\Phi_{n+1}+\Phi_{n-1})+Fdn\Phi_n$, with hopping constant J, and tilting potential Fdn. In the absence of disorder and interactions, the particles perform BOs with frequency $\omega_{BO}=Fd/\hbar$, and amplitude $z_{BO}=2Jd/\hbar\omega_{BO}$. The eigenstates of $\hat{H}_0$ are the WS states [19], $|W_m\rangle=\Sigma_n J_{n-m}|n\rangle$, where $J_n\equiv J_n(z_{BO})$ is the Bessel function of first kind. The eigenenergies form the well-known WS ladder $E_m^0=m\hbar\omega_{BO}$. We project the DNLSE in the WS basis $\psi_m\equiv\langle W_m|\Phi\rangle$,

$$i\hbar\dot{\psi}_m = E_m^0\psi_m + \sum_{m'} B_{mm'}\psi_{m'} + \sum_{m',s,s'} A_{m,m'}^{s,s'}\psi_{m'}^*\psi_{s'}\psi_s, \tag{4}$$

where

$$B_{mm'} \equiv \sum_n \epsilon_n J_{n-m}J_{n-m'},$$

and

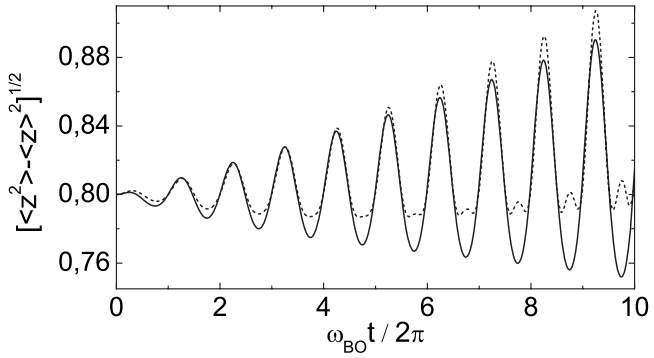

FIG. 2. Condensate width in units of z_{BO} obtained from direct simulation of Eq. (1) (dashed) and from the WS analysis discussed in the text (solid), for $\hbar\omega_{BO}=0.08J$, $U/\hbar\omega_{BO}=3.7$, and $\epsilon_n/\hbar\omega_{BO}=0.1\cos 0.16\pi n$.

$$A_{m,m'}^{m'',m'''} \equiv U\sum_n J_{n-m}J_{n-m'}J_{n-m''}J_{n-m'''}.$$

If $\hbar\omega_{BO}$ is much larger than other energy scales we can neglect terms in Eq. (4) that introduce energy jumps larger than $\hbar\omega_{BO}$, i.e., we can employ rotating-wave-approximation (RWA) arguments. In the RWA the disorder preserves $\rho_m \equiv |\psi_m|^2$, just providing a shift $E_m^0+B_{mm}$. Note that on a longer time scale of several BOs the RWA may fail and the disorder eventually leads to a transfer of population between WS states. The interactions can, even in the RWA, lead to a transfer of population between WS states. However, since $\dot{\rho}_m \sim \rho_m^2$, whereas the phase φ_m of ψ_m evolves as $\dot{\varphi}_m \sim \rho_m$, we may consider ρ_m as being constant (at least at short time scales of few BOs) if the atomic wave packet is sufficiently broad [23]. In that case, the energy of the WS states becomes

$$E_m \simeq m\hbar\omega_{BO} + B_{mm} + 2\sum_n (\Gamma_n^e\rho_{m-2n} + \Gamma_n^0\rho_{m-2n-1}), \tag{5}$$

with $\Gamma_n^e \equiv A_{n,n}^{n,n}$, and $\Gamma_n^0 \equiv A_{n+1,n}^{n+1,n}$. Hence, the energies of the WS states are not equidistantly spaced, the wave packet undergoes dephasing, and as a consequence the BOs are damped. In addition, the BEC width experiences a breathing dynamics [23], as shown in Fig. 2. This figure shows (at least during the first BOs) a good agreement between our results from a direct simulation according to Eq. (3) and those obtained using WS states $\psi_m(t)=\sqrt{\rho_m(0)}e^{-iE_m t/\hbar}$, where E_m is given by Eq. (5).

Let us now discuss the intriguing role of the interactions on the BOs in more detail. In the lower panel of Fig. 1, a stronger damping than in the single particle case can be observed for large nonlinearity (see the curve for $N=700$). This interaction-induced damping is related to the so-called dynamical instability [20,22]. This instability occurs when the quasimomentum reaches the outer parts of the Brillouin zone and small perturbations of the condensate wave function grow exponentially in time [21]. This mechanism becomes predominant with growing nonlinearity, strongly damping the BOs.

On the contrary, the BO damping may be significantly reduced compared to the single particle case for weak nonlinearity (see the curve for $N=350$). This effect is caused by

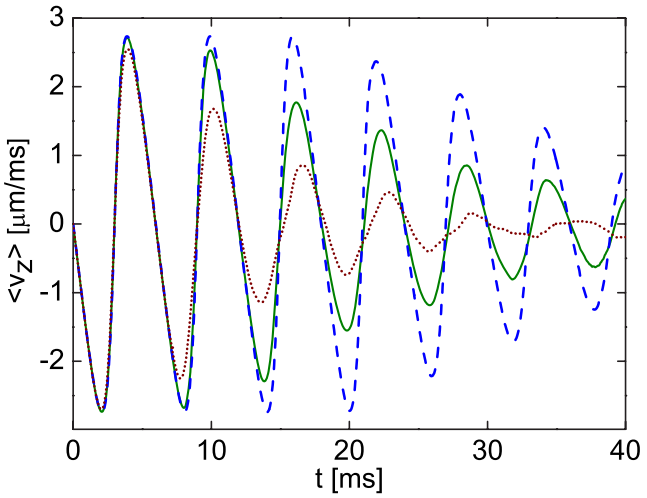

FIG. 3. (Color online) Expectation value of the axial velocity for disorder depths 0 (dashed), $0.02E_r$ (solid), and $0.06E_r$ (dotted), for the 3D example discussed in the text.

an interaction-induced *dynamical screening of the disorder* [24] and can be qualitatively better understood with an alternative semiclassical description of the BOs. In the regime of weak nonlinearity, we can assume that the dynamics occurs within the lowest Bloch band, and that the dynamical instability is irrelevant on the time scales considered. Let us denote the exact mean-field potential obtained by solving the GPE (1) by $V_{mf}(z,t)=g|\Phi(z,t)|^2$, and consider the effective single particle problem, for a particle in the lowest Bloch band under the influence of $V_{mf}(z,t)$, the tilting force F, and the disorder $V_{dis}(z)$. The single particle Hamiltonian is given by $H_{eff}=-2J\cos(\hat{k}d)-F\hat{z}+V_{dis}(\hat{z})+V_{mf}(\hat{z},t)$. In the quasimomentum picture, $\hat{k}\rightarrow k$, and $\hat{z}=i\partial/\partial k$. We assume that the bare amplitude of the BOs, z_{BO}, is much smaller than the spatial spread of the initial wave function. This in turn implies a very narrow initial momentum distribution, centered at k_0, so that, in the absence of disorder and nonlinearity (zero-order solution), $\hat{z}(t)\simeq\hat{z}(0)-z_{BO}\cos[(Ft/\hbar+k_0)d]$. The full Heisenberg equation for $\hat{k}$ reads $d\hat{k}/dt=F-(\partial V_{dis}/\partial z)\times(\hat{z})-(\partial V_{mf}/\partial z)(\hat{z},t)$. We solve it perturbatively by inserting the zero order solution. Again, assuming a sharp initial momentum distribution we obtain $\hat{z}(t)\simeq\hat{z}(0)-z_{BO}\cos\{\frac{Ftd}{\hbar}+k_0d-\frac{d}{\hbar}\int_0^t dt'[(\partial V_{dis}/\partial z)(\hat{z})-(\partial V_{mf}/\partial z)(\hat{z},t')]\}$. In order to calucalte the dephasing rate the latter expression has to be averaged over the initial spread of $\hat{z}(0)$. A reasonable estimate of the rate is $\gamma^2\simeq\frac{d^2}{\hbar^2t^2}\langle\{\int_0^t dt'[(\partial V_{dis}/\partial z)(\hat{z}(0))+(\partial V_{mf}/\partial z)(\hat{z}(0),t')]\}^2\rangle$. Note that, when acting alone, both disorder and nonlinearity lead to the damping of the BOs. However, when acting together, they may compensate each other if the product of the time averaged forces due to disorder and nonlinearity averaged over $\hat{z}(0)$ is negative, qualitatively explaining the dynamical screening of the disorder observed in Fig. 1.

In the previous discussion we have constrained our analysis to the somewhat simplified quasi-1D regime, where the xy dynamics is absent. However, typical experiments are not performed in this regime, and transversal excitations of the

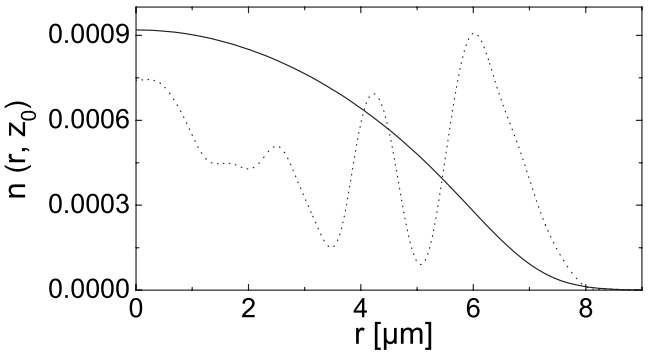

FIG. 4. Radial density profiles at the axial position z_0 of maximal density, at $t=0$ (solid), 16 ms (dotted), for the case discussed in the text.

condensates may significantly alter the BO dynamics. Hence a quantitative description of the BOs demands a three-dimensional GPE simulation. We maintain a cylindrical trap, and hence we simplify our 3D calculations by assuming cylindrical symmetry of the wave function around the z axis. Since experiments typically detect BOs by observing the velocity distribution, we analyze the expectation value of the axial velocity $\langle v_z\rangle=\int d^3r\Phi^*\frac{\hbar}{im}\partial_z\Phi$. Figure 3 shows the case of $N=5\times10^4$ particles, for the same lattice tilting considered

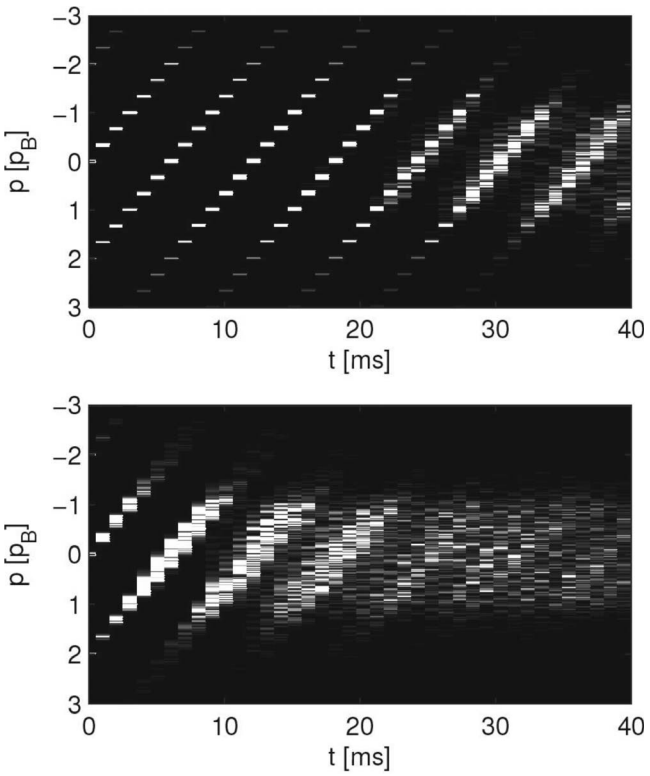

FIG. 5. Gray-scale plot of the momentum distribution $n(p_\perp=0,p_z)$, calculated every 1 ms during the BOs. The upper panel shows the nondisordered case, the lower panel shows the result for a disorder depth of $0.06E_r$. The pictures correspond to the 3D configuration of Figs. 3 and 4. This momentum distribution directly corresponds to the outcome of a TOF measurement and thus shows the expected experimental signature of the disorder induced effects.

before, but for trap frequencies $\omega_z = 2\pi \times 14$ Hz, $\omega_\perp = 2\pi \times 35$ Hz, lattice depth $s=2$, and a disorder potential of depth $V_\Delta = 0.02E_r$ and correlation length $L \simeq 10$ μm. These parameters are well attainable experimentally [12], and hence our simulations show that the damping of BOs can be studied under realistic conditions. For the large number of atoms considered here, damped BOs are observed even in the absence of disorder due to a fast damping by the dynamical instability. Under these conditions our 3D results clearly deviate from the expected quasi-1D results, due to the development of a complex radial dynamics shown in Fig. 4, due to instability of the radial excitations. Hence although the dynamical instability is also encountered in one dimension, the full computation of the dynamics does require the careful consideration of the radial degree of freedom.

Finally, we discuss a method for the experimental observation of damped BOs. A direct measurement of the damping in position space constitutes a very difficult task, since the oscillation amplitude is typically too small for an *in situ* measurement. TOF measurements provide a much better method. Due to the very fast decrease of the mean-field energy during the TOF, the expanded density distribution provides an approximate image of the momentum distribution $n(\vec{p})$ of the sample at the moment of release. Figure 5 shows the momentum distribution at various stages during the BOs. In the absence of disorder, the quasimomentum q scans the Brillouin zone due to the acceleration introduced by the tilting force $(\dot{q} = F/\hbar)$ [19]. Consequently, the population of the different momentum components changes, resulting in a coherent oscillation of the mean momentum. The spectrum consists of several sharp peaks, which are separated from each other by the lattice momentum $p_B = 2\hbar\bar{k}$. Hence the density distribution after an expansion time τ consists of several small clouds, well separated from each other by $\Delta z = 2p_B\tau/m$. This picture changes when disorder is introduced to the system. The initial sharp momentum components are progressively broadened, eventually reaching an irregular occupation of momenta. This broadening originates from the irregular energy spacing of the WS states and leads to a broadened density distribution after TOF. Note that on long time scales, a significant broadening of the momentum components is also introduced by the interactions in the absence of disorder, as shown in Fig. 5. However, a very clear distinction between the ordered and disordered case is possible on time scales of up to a few BO periods. Moreover, our 3D simulations of the expansion dynamics show that it is possible to observe a clear separation between the center of mass position for the ordered and disordered lattices under realistic conditions, due to the differences in the expected value of the momentum in both cases (Fig. 3). Also note that Fig. 5 shows the axial momentum distribution for zero transversal momentum, which is significantly reduced during the time evolution. This reflects the previously mentioned excitation of transverse modes.

In summary, both disorder and interactions separately lead to BO damping. However, when acting simultaneously the interactions may partially screen the disorder, leading to a reduction of the BO damping. We have shown that the interplay of disorder and interactions may be observed under realistic experimental conditions by monitoring the evolution of the momentum distribution of the system. Although we were mainly interested in disordered lattices, similar results may be obtained for lattices in the presence of inhomogeneous forces, as, e.g., spatially inhomogeneous Casimir-Polder forces close to surfaces. It has recently been proposed that the frequency shift of BOs of lattice fermions can be an excellent way of measuring such tiny forces [25]. The monitoring of BO damping and the sample width may provide an excellent way of proving the inhomogeneity of these forces.

We thank L. Sanchez-Palencia for fruitful discussions. We acknowledge support from the programs QUDEDIS (Grants No. 1365 and No. 1551) and Euroquam FERMIX of the European Science Foundation (ESF). This work was supported by the Deutsche Forschungsgemeinschaft (SFB 407, SFB-TR21, SPP1116), and Spanish MEC (FIS 2005-04627, Consolider Ingenio 2010 QOIT).

[1] See, e.g., N. W. Ashcroft and N. D. Mermin, *Solid State Physics* (Saunders, Philadelphia, 1976).
[2] F. Bloch, Z. Phys. **52**, 555 (1928); C. Zener, Proc. R. Soc. London, Ser. A **145**, 523 (1934).
[3] C. Waschke, H. G. Roskos, R. Schwedler, K. Leo, H. Kurz, and K. Kohler, Phys. Rev. Lett. **70**, 3319 (1993).
[4] M. Ben Dahan, E. Peik, J. Reichel, Y. Castin, and C. Salomon, Phys. Rev. Lett. **76**, 4508 (1996); S. R. Wilkinson, C. F. Bharucha, K. W. Madison, Q. Niu, and M. G. Raizen, *ibid.* **76**, 4512 (1996); O. Morsch, J. H. Muller, M. Cristiani, D. Ciampini, and E. Arimondo, *ibid.* **87**, 140402 (2001); G. Roati, E. deMirandes, F. Ferlaino, H. Ott, G. Modugno, and M. Inguscio, *ibid.* **92**, 230402 (2004).
[5] L. Guidoni, C. Triché, P. Verkerk, and G. Grynberg, Phys. Rev. Lett. **79**, 3363 (1997); G. Grynberg, P. Horak, and C. Mennerat-Robilliard, Europhys. Lett. **49**, 424 (2000).
[6] B. Damski, J. Zakrzewski, L. Santos, P. Zoller, and M. Lewenstein, Phys. Rev. Lett. **91**, 080403 (2003).
[7] R. Roth and K. Burnett, J. Opt. B: Quantum Semiclassical Opt. **5**, S50 (2003); R. Roth and K. Burnett, Phys. Rev. A **67**, 031602(R) (2003).
[8] U. Gavish and Y. Castin, Phys. Rev. Lett. **95**, 020401 (2005).
[9] T. Schulte, S. Drenkelforth, J. Kruse, R. Tiemeyer, K. Sacha, J. Zakrzewski, M. Lewenstein, W. Ertmer, and J. J. Arlt, New J. Phys. **8**, 230 (2006).
[10] J. E. Lye, L. Fallani, M. Modugno, D. S. Wiersma, C. Fort, and M. Inguscio, Phys. Rev. Lett. **95**, 070401 (2005).
[11] D. Clément, A. F. Varon, M. Hugbart, J. A. Retter, P. Bouyer, L. Sanchez-Palencia, D. M. Gangardt, G. V. Shlyapnikov, and A. Aspect, Phys. Rev. Lett. **95**, 170409 (2005); C. Fort, L. Fallani, V. Guarrera, J. E. Lye, M. Modugno, D. S. Wiersma, and M. Inguscio, *ibid.* **95**, 170410 (2005).
[12] T. Schulte, S. Drenkelforth, J. Kruse, W. Ertmer, J. Arlt, K. Sacha, J. Zakrzewski, and M. Lewenstein, Phys. Rev. Lett. **95**,

170411 (2005).
[13] S. Ospelkaus, C. Ospelkaus, O. Wille, M. Succo, P. Ernst, K. Sengstock, and K. Bongs, Phys. Rev. Lett. **96**, 180403 (2006).
[14] L. Fallani, J. E. Lye, V. Guarrera, C. Fort, and M. Inguscio, Phys. Rev. Lett. **98**, 130404 (2007).
[15] J. E. Lye, L. Fallani, C. Fort, V. Guarrera, M. Modugno, D. S. Wiersma, and M. Inguscio, Phys. Rev. A **75**, 061603(R) (2007).
[16] A similar dynamical screening may explain some features observed in dipole oscillations in Ref. [15].
[17] L. Pitaevskii and S. Stringari, *Bose-Einstein Condensation* (Clarendon Press, Oxford, 2003).
[18] S. A. Trombettoni and A. Smerzi, Phys. Rev. Lett. **86**, 2353 (2001), and references therein.
[19] T. Hartmann, F. Keck, H. J. Korsch, and S. Mossmann, New J. Phys. **6**, 2 (2004).
[20] L. Fallani, L. De Sarlo, J. E. Lye, M. Modugno, R. Saers, C. Fort, and M. Inguscio, Phys. Rev. Lett. **93**, 140406 (2004).
[21] M. Modugno, C. Tozzo, and F. Dalfovo, Phys. Rev. A **70**, 043625 (2004).
[22] C. Menotti, A. Smerzi, and A. Trombettoni, New J. Phys. **5**, 112 (2003).
[23] D. Witthaut, M. Werder, S. Mossmann, and H. J. Korsch, Phys. Rev. E **71**, 036625 (2005).
[24] Note that the related interaction-induced *static screening effect* is responsible for washing out Anderson localization in BECs (see, e.g., [12], and references therein).
[25] I. Carusotto, L. Pitaevskii, S. Stringari, G. Modugno, and M. Inguscio, Phys. Rev. Lett. **95**, 093202 (2005).